

Study of Early-Age Creep and Shrinkage of Concrete Containing Iranian Pozzolans: An Experimental Comparative Study

P. Ghodousi¹, M.H. Afshar^{1,*}, H. Ketabchi² and E. Rasa³

Abstract. *This paper presents an experimental study on prediction of the early-age creep and shrinkage of concrete with and without silica fumes, trass, ground-granulated blast-furnace slag, combinations thereof, and influences of the proposed Iranian pozzolans. Experiments were carried out under a controlled ambient condition at a temperature of 40° C and a relative humidity (RH) of 50%, and a laboratory ambient condition at a temperature of 20° C and a relative humidity (RH) of 30% in order to collect the required data. Comparisons are made between ACI209-92, BS8110-1986 and CEB1970 prediction models, and an estimation model, based on 28-day results (short-term test method), using the same experimental data to predict the creep and shrinkage of the specimens at the ages of 120 and 200 days after curing. The results show that the above-mentioned models are not accurate enough for predicting the creep and shrinkage of concrete containing local Iranian pozzolans. It was also observed that the prediction, based on short-term results, would lead to more accurate creep and shrinkage predictions.*

Keywords: *Creep; Pozzolanic concrete; Prediction models; Short-term test method; Shrinkage; Silica fume; Ground-granulated blast-furnace slag; Trass.*

INTRODUCTION

The time-dependant deterioration of concrete is a persistent problem arising from rapid complex volume changes such as creep and shrinkage which, in turn, leads to the development of stresses in the material. The creep and shrinkage of concrete are mainly due to water migration, chemical processes and the displacement of gel particles taking place on the micro level of the hardened cement paste [1,2].

Shrinkage, the decrease of concrete volume with time after the hardening of concrete, is due to changes in the moisture content of concrete and the physical-chemical changes that occur without stress. Shrinkage

is conveniently expressed as a dimensionless strain [2,3]. Three mechanisms of concrete shrinkage may be distinguished as 1) capillary; 2) chemical; and 3) drying. Capillary shrinkage is the result of capillary pressure produced by the surface tension of water in fresh concrete during the early hours of drying. Chemical shrinkage (or swelling) is caused by a number of chemical processes such as hydration shrinkage, thermal shrinkage, dehydration shrinkage, crystallization swelling, carbonation shrinkage and conversion shrinkage. Drying shrinkage, probably the most significant contributor to macroscopic dilation, is caused by the migration of water from pores and capillaries. Drying shrinkage is usually described with a diffusion model. Microcrack formation and internally created stresses produce creep, modify the time-dependent deformation and result in a complex nonlinear diffusion process [4].

The time-dependent increase of strain in hardened concrete subjected to sustained stress in excess of shrinkage is defined as creep. Creep includes basic creep and drying creep. Basic creep occurs under conditions where there is no moisture movement to or

1. Department of Civil Engineering, Iran University of Science and Technology, Narmak, Tehran, P.O. Box 16765-163, Iran.

2. Department of Civil Engineering, Sharif University of Technology, Tehran, P.O. Box 11155-9313, Iran.

3. Department of Civil and Environmental Engineering, University of California, Davis, One Shield Ave., Davis, CA 95616, USA.

*. Corresponding author. E-mail: mhafshar@iust.ac.ir

Received 22 November 2006; received in revised form 26 November 2007; accepted 16 June 2008

from the environment. Drying creep is the additional creep caused by drying. Creep coefficient, the ratio of the creep strain to the initial elastic (instantaneous) strain due to a sustained stress, is commonly used as a measure of creep deformation. As a time-dependent property, creep has a similar impact on the behavior of pre-stressed concrete members such as shrinkage strains [2,3]. Two mechanisms of creep in the absence of drying may be distinguished: short-term creep and long-term creep. Short-term creep is a consequence of the redistribution of capillary water within the structure of the hardened cement paste, while long-term creep is due to the displacement of gel particles under load and, to a lesser extent, to the creep of gel particles. Simultaneous drying further complicates the process, because the sum of instantaneous and creep deformation is larger than the sum of creep and shrinkage deformations measured separately. In analysis and design, creep is usually accounted for by using a creep factor, i.e. the ratio of creep strain at any time to instantaneous strain [4].

Two different approaches are currently being used for predicting the creep and shrinkage of concrete: 1) An empirical approach, in which time functions are determined from a number of tests by curve-fitting, and 2) An analytical approach in which time functions are obtained by solving differential equations of postulated processes governing the creep and shrinkage behavior. In either case, the model parameters are obtained by calibrating the model using the number of test results available. There are three popular models for the prediction of creep and shrinkage of concrete, namely; 1) ACI209-92 [5]; 2) BS8110-1986 [6]; and 3) CEB1970 [7]. The short-term test method [8], an estimation using 28-day results, is another method for predicting the creep and shrinkage of concrete.

There are other prediction models for the creep and shrinkage of concrete. The GZ is a model that includes the effects of ambient relative humidity, the strength of concrete at 28 days, the drying age after moist curing and the member size. This model, however, does not take into account the effects of rapidly developed early-age creep and shrinkage, which are especially important to HPC [9]. The B3 model is another model that has received some publicity in the literature in recent years. The B3 model is based on the material behavior phenomenological theory. Instead of using a creep coefficient, the model utilizes a compliance function that may reduce the risk of errors due to incorrect modulus values. The use of the B3 model, however, has been judged as relatively complex and questions have been raised regarding its suitability for practicing engineers. In addition, the B3 models of shrinkage and creep may require input data that is not generally available at the time of design [10]. The BP-KX model is based on an analytically derived

time function and empirically determined parameters. The BP-KX model is more cumbersome to use, but it provides a better fit to the test results. Obviously, predictions can be improved from short-term measurements of creep and shrinkage [11].

Vandewalle [12] studied the creep and shrinkage of concrete under both constant and variable ambient conditions. The Relative Humidity (RH) and temperature at which the concrete is cast have been reported to be of great influence on its basic creep, total creep and drying shrinkage, whereas the effect of the cyclic variation in RH was not significant. Sharon Hou et al. [13] investigated creep, shrinkage and the modulus of elasticity of HPC mixtures with local materials. The test results showed that the current ACI equations for shrinkage, creep, and the modulus of elasticity of concrete do not accurately predict these material properties for HPC. Neville, Dilger, Brooks and Bamforth [14] studied the basic creep of slag concretes. Results showed that the higher the slag replacement percentage, the lower the level of basic creep. Whiting, Detwiler, and Lagergren [15] investigated the drying shrinkage and cracking tendency of silica fume concrete for bridge deck applications. They reported that concrete containing silica fume showed greater early-age drying shrinkage than plain concrete, but the use of silica fume had little influence on the long-term shrinkage of concrete. Ojdrovic et al. [16] presented a method for predicting the ultimate creep and shrinkage from the results of short-term standard creep and shrinkage tests on 5 cm diameter cylinders. Such predictions were compared with the results of long-term creep and shrinkage tests. Results showed that the accuracy of prediction of the ultimate creep and shrinkage increases significantly when short-term test results are used to adjust the models. Li et al. [17] reported a study on the early-age creep and shrinkage of concrete with and without silica fume, ground granulated blast-furnace slag and combinations thereof. The compressive and tensile creep strains together with drying and autogenous shrinkage were determined over 4 months of loading. The results obtained for plain, double-blended and triple-blended concrete were assessed and compared to provide guidelines on the use of silica fume and slag in concrete structures subjected to early-age creep and shrinkage.

In the present paper, the main results of a set of experimental creep and shrinkage tests on concrete specimens under two different ambient conditions at sustained loading are presented. The influence of silica fume, trass and ground-granulated blast-furnace slag with different replacement percentages and curing conditions, on the creep and shrinkage behavior of concrete, is investigated. In this study, ACI209-92, BS8110-1986 and CEB1970 prediction models and an

estimation based on 28-day results are conducted and the predictions are compared with experimental results for the series at 120 and 200 days after curing.

EXPERIMENTAL PROGRAM

Materials

Three types of cement, namely, ASTM type II Portland cement, blended slag cement and blended trass cement were used in this study. Silica fume was used as a supplementary cementitious material in some mixtures. The physical properties and chemical composition of these materials are presented in Tables 1 to 3. Natural gravel with a maximum size of 12.5 mm and natural sand were used as the aggregates of the mixtures. The physical properties of aggregates are presented in Table 4.

The gradation of aggregates is presented in Figure 1a and Figure 1b, satisfying ASTM C33. A superplasticizer with the commercial name of Melcrete was used to obtain the required workability. To assure uniformity of supply, the materials were subjected to periodical control tests.

Mixture Proportion and Curing Condition

The mixture proportions are presented in Table 5. The first letter of each mixture code represents the cement and pozzolan type while the second letter indicates the ambient condition under which the specimens were stored. After casting, all of the specimens were covered with wet burlap at laboratory conditions of 20°C and 30% relative humidity and demolded after 48 hours. The specimens were then moist-cured and stored for 28 days at 20°C. Two different ambient conditions used

Table 1a. Chemical properties of cement.

Chemical Analysis	Portland Type II	Slag Cement
Silicon dioxide (SiO ₂)%	20.79	26.3
Aluminium oxide (Al ₂ O ₃)%	4.53	8.3
Ferric oxide (Fe ₂ O ₃)%	3.81	2.1
Calcium oxide (CaO)%	63.18	55.8
Magnesium oxide (MgO)%	2.78	4.2
Sulfur trioxide (SO ₃)%	2.02	1.8
Potassium oxide (K ₂ O)%	0.57	0.76
Loss on ignition (LOI) %	2.02	0.3
Insoluble residue%	0.43	0.2
Free CaO%	1.01	-
Tricalcium silicate (C ₃ S)%	57.34	-
Dicalcium silicate (C ₂ S)%	15.93	-
Tricalcium aluminate (C ₃ A)%	5.89	-
Calcium alumino ferrita % (C ₄ AF)	10.98	-

Table 1b. Physical properties of cement.

Physical Tests	Portland Type II	Slag Cement
Fineness, Blaine test, (cm ² /gr)	2383	3300
Retained on sieve #70	-	-
Retained on #170%	3	-
Autoclave expansion%	0.22	0.08
Water for normal consistency%	26	-
Setting time, Vicat test, initial (minutes)	150	-
Setting time, Vicat test, final (minutes)	180	-
Compressive strength (kg/cm ²) 3 days	201	112
Compressive strength (kg/cm ²) 7 days	295	175
Compressive strength (kg/cm ²) 2 8days	413	290

Table 2. Chemical and physical properties of silica fume.

Particle Size (μm)	< 1
Specific Gravity	2.2
Surface Area (BET) (m^2/kg)	15,000-30,000
SiO₂ Content%	85- 97
Loss on Ignition%	5

Table 3. Trass properties.

Loss on Ignition (LOI)%	9.52
(SiO₂)%	68.54
(Al₂O₃)%	12.75
(MgO+CaO)%	3.72
(SO₃)%	0.8
(CO₂)%	3.37
Cl%	0.35
(K₂O+Na₂O)%	2.68

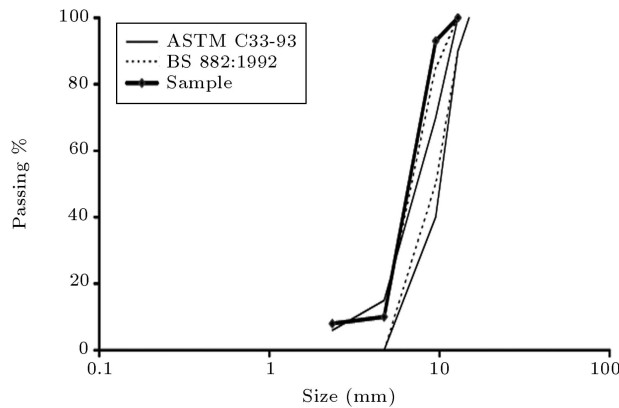


Figure 1a. Gradation curve of coarse aggregate.

for the creep and shrinkage specimens were laboratory conditions and a controlled condition of 20°C and 30% relative humidity, and 40°C and 50% relative humidity, respectively.

Test Program

For each test, two specimens were tested. Table 6 shows the concrete specimen dimensions used for each of the tests. Three types of specimen, namely 100 mm cubes, 150×100 mm cylinders and 80×80 mm

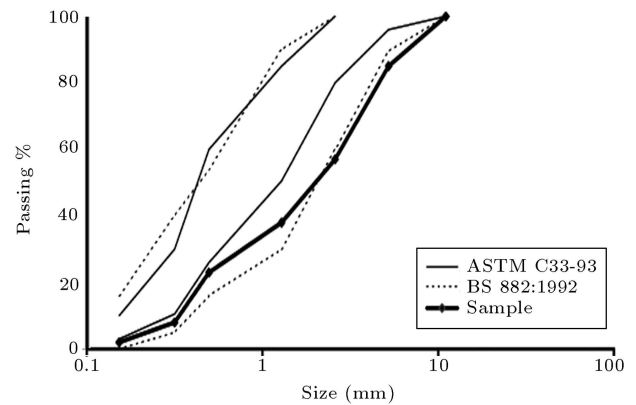


Figure 1b. Gradation curve of fine aggregate.

cylinders were used to perform the compression tests. The compressive strength of each mixture was used for calculation of the load to be applied to the compressive creep specimens, which was taken as 33% of the average compressive strength. The specimen preparation and testing for the modulus of elasticity followed the ASTM C469. The modulus of elasticity was measured using 150×300 mm cylinder specimens and electronic strain gauges. The modulus of elasticity was determined at the third loading. The experiment on creep specimens was conducted at the same time as the shrinkage specimens. Creep specimens were cast at the same time and cured for the same duration as that of the corresponding shrinkage specimens. The shrinkage strains of concrete specimens were measured using two 75×75×285 mm prisms and two 80×210 mm cylindrical specimens. The shrinkage test procedure followed the guidelines of the ASTM C490. In order to measure cylindrical specimen shrinkage, a pair of special steel bolts was installed in both sides of the specimens and the shrinkage strain was measured at the desired times. The shrinkage of each specimen was taken as the mean of the recorded shrinkage values of each side. Each frame was considered for one 80×280 mm cylindrical specimen installation. To measure the shrinkage of each specimen, two specimens and two shrinkage frames were adopted. Bolts and rivets on top of the frames were used to apply stress and a spring at the bottom of the frames was used to prevent the load from being decreased. The stress was controlled by use of a load cell. A pair of steel bolts on each side of the concrete specimen was installed to measure the amount of creep strain at the

Table 4. Physical properties of aggregates.

Aggregate Type	Water Absorption%	Density(gr/cm^3) (in SSD Condition)	Passing No. 200 Sieve Size
Fine	4.07	2.5	2
Coarse	3.1	2.54	1

Table 5. Mixture proportion.

Concrete Code	Water-Cementitious Materials	Cement (kg/m ³)	Pozzolan		Fine	Coarse Aggregate (kg/m ³)	Super Plasticizer (kg/m ³)	Environmental Condition
			Type	Content (kg/m ³)	Aggregate (kg/m ³)			
PL	0.43	400	-	-	796	972	1.1	Lab.
PC1	0.43	400	-	-	796	972	1.2	Controlled
SFL	0.43	372	Silica Fume	28	796	972	1.5	Lab.
SFC1	0.43	372	Silica Fume	28	796	972	1.5	Controlled
SFC2	0.55	272	Silica Fume	28	796	972	-	Controlled
TL	0.43	400	Trass	25% mixed	796	972	1.18	Lab.
TC	0.43	400	Trass	25% mixed	796	972	1.5	Controlled
SC1	0.43	400	Slag	30% replacement	796	972	1.2	Controlled
SC2	0.43	400	Slag	15% replacement	796	972	1.46	Controlled

Table 6. Specimens dimensions.

Test Type	Specimens Type	Specimens Dimensions (mm)
Density of fresh concrete	Cylindrical	150×300 ^(a)
Compressive strength	Cubic	100×100
	Cylindrical	150×300 ^(a)
	Cylindrical	80×280 ^(b)
Modulus of elasticity	Cylindrical	150×300 ^(a)
Shrinkage	Cylindrical	80×210
	Prismatic	75×75×285
Creep	Cylindrical	80×280 ^(b)

(a)The 150×300 cylindrical specimen was made for controlling of relation between the cubic and cylindrical specimens.

(b)The 80×280 cylindrical specimen was made for determination of the loading amount.

desired times. Strains measured immediately upon loading were considered as elastic strains, neglecting the fact that some creep, normally not exceeding 5 min, could have occurred during this period. Deformations were then recorded as the total deformation of creep specimens. Since the creep specimens were exposed to the same environmental conditions as the shrinkage specimens, creep strains could be determined directly by subtracting the average strain of the shrinkage specimens from the total strains of the creep specimens

without considering any effects of the temperature and relative humidity.

RESULTS AND DISCUSSION

The slump, density, 28-day compressive strength and modulus of elasticity, as obtained for the nine concrete mixtures, are presented in Table 7. The 28-day compressive strength of the concrete mixtures was determined using cube specimens of 100×100×100

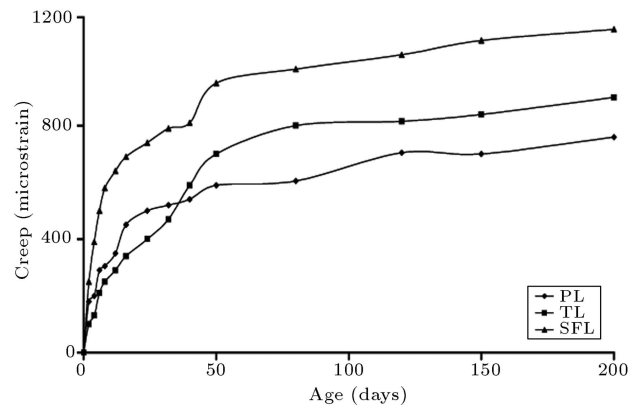
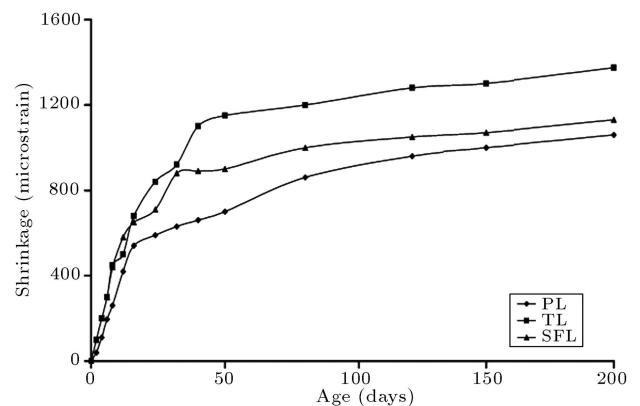
Table 7. Concrete properties.

Concrete Code	Slump (mm)	Density (kg/m ³)	Compressive Strength (MPa)	Modulus of Elasticity (GPa)
PL	30	2273	37.5	26
PC1	40	2352	39	27
SFL	32	2310	48	34
SFC1	35	2330	50	35
SFC2	32	2292	40	16
TL	35	2280	29	18
TC	30	2290	31	19
SC1	34	2360	34.5	17
SC2	40	2370	45.5	20

mm. The results indicated that concrete containing silica fume (SFC1) exhibited the highest compressive strength (50 MPa) and concrete containing trass (TL) exhibited the lowest compressive strength (29 MPa).

The test results of creep and shrinkage specimens in some HPC mixtures are presented in this section. Due to space limitation, only the results of three groups of creep and shrinkage specimens are discussed here. 200-day creep and shrinkage of PL, SFL and TL concrete mixtures, under laboratory ambient condition, are presented in Figures 2a and 2b. As with plain concrete (PL), a high initial rate of creep and shrinkage was observed in approximately the first 30 days of loading and the rate was sensitive to age during loading at a very early age. The age-sensitivity of the creep and shrinkage rate was reduced by increasing age, creep and shrinkage becoming approximately age-independent after 100 days. The creep and shrinkage strains for PL at a loading age of 200 days were 760 and 1100 microstrains, respectively. It is clear from Figures 2a and 2b that silica fume concrete, namely SFL, shows a higher creep and shrinkage than PL under similar conditions. The creep and shrinkage strains of SFL were measured as 1160 and 1130 microstrains at this age, respectively. At the very early ages, approximately 40 days, the creep values of TL were lower than PL, but at the higher ages it was vice-versa. The 200-day creep value of TL was recorded as 900 microstrains. The shrinkage obtained under this condition increased with the age of loading up to approximately 40 days and, thereafter, had a lower rate up to 200 days; TL exhibited the highest shrinkage strains. It is worth mentioning that silica fume concrete (SFL) exhibited the greatest creep and plain concrete (PL) exhibited the lowest creep strain among all the concrete mixtures under laboratory ambient conditions.

Figures 3a and 3b present the result of creep and shrinkage for plain concrete (PC1), silica fume concrete (SC1) and

**Figure 2a.** 200-day creep of concretes in laboratory condition.**Figure 2b.** 200-day shrinkage of concretes in laboratory condition.

blended cement concrete containing slag mixtures, respectively, under controlled ambient conditions at the age of 200 days. As shown in Figures 3a and 3b, the creep and shrinkage strains under controlled conditions increase rapidly with the age of loading up to approximately 50 days, after which they remain nearly constant up to the end of the test at 200

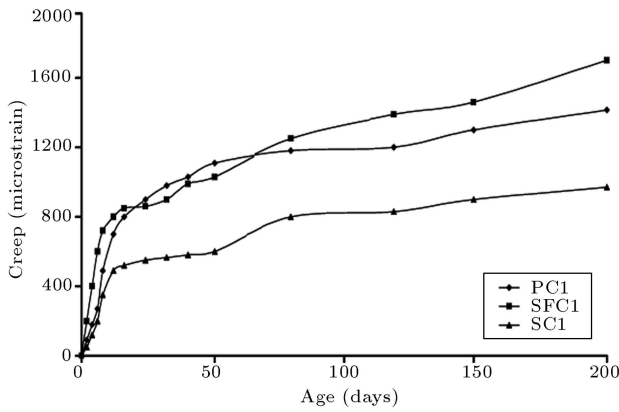


Figure 3a. 200-day creep of concretes in controlled condition.

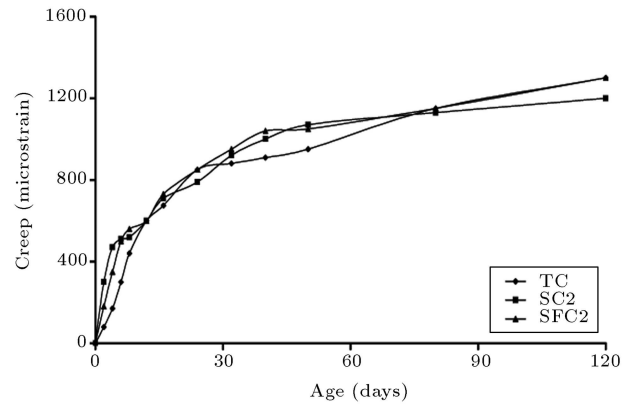


Figure 4a. 120-day creep of concretes in controlled condition.

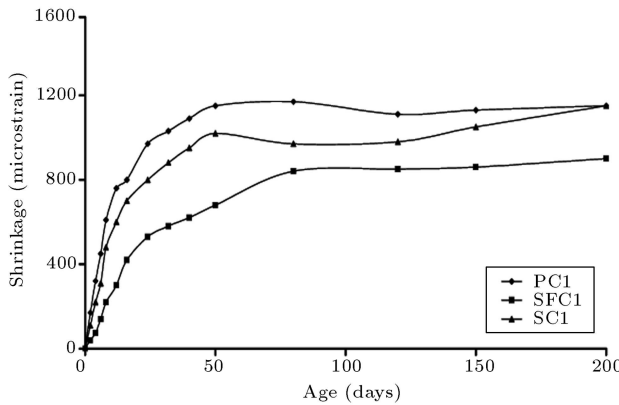


Figure 3b. 200-day shrinkage of concretes in controlled condition.

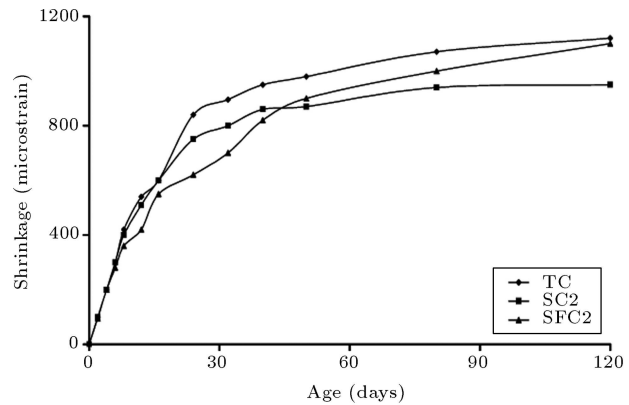


Figure 4b. 120-day shrinkage of concretes in controlled condition.

days. Values of creep and shrinkage reached 1425 and 1180 microstrains at the age of 200 days for PC1, respectively. It is noteworthy that SFC1, with higher creep strains, showed less shrinkage than PC1 and SC1 within ages of less than 200 days. The value of creep for SC1 at the end of the test (200 days) reached 1300 microstrains. SC1 had lower creep strains within the test duration in comparison to PC1 and SFC1. After 200 days, the SC1 specimens shrank by 1150 microstrains, while the shrinkage of PC1 was by 1180 during the same time.

The creep and shrinkage strains of TC, SC2 and SFC2 were plotted against the age of loading in Figures 4a and 4b under controlled ambient conditions, respectively. It is seen that, under these conditions, the creep and shrinkage of all the concrete specimens increased continuously up to 120 days. It was noted that a high initial rate of creep and shrinkage was seen in approximately the first 40 days. At the age of 120 days, the creep strains of TC and SFC2 were higher than PC1, but the creep values of SC2 were lower than that of PC1. The shrinkage values of TC, SFC2 and SC2 were lower than PC1, but the differences were not considerable.

Furthermore, some remarks should be made here regarding the results of creep and shrinkage strains under controlled ambient conditions. It can be observed from Figures 3a and 3b and Figures 4a and 4b that blended cement concrete containing 30% slag replacement (SC1) had the lowest creep and silica fume concrete (SFC2) exhibited the highest creep. Creep of SC2 containing 15% slag replacement was higher than that for SC1 containing 30% slag replacement, even though shrinkage takes place in the opposite direction to creep. It was shown earlier that higher slag content leads to lower creep and higher shrinkage strains.

Fulton [18] and Hogan and Meusel [19] reported an increase in drying shrinkage when various blends of ground-granulated blast-furnace slag were used as compared with plain concrete. This is opposite to the observation made in this study (Figure 3b), particularly for SC2 (up to 120 Days). On the other hand, Klinger and Isberner [20] found little difference in drying shrinkage when slag concrete was compared with normal Portland cement concrete alone, which is in line with the outcome of the current investigation. This is to be expected, considering that SFC2 had a higher

water-cementitious materials ratio ($W/cm=0.55$) that might cause greater strains of creep from concrete; creep is generally thought to increase with a water-cementitious materials ratio [21]. It is found that slag was more effective in decreasing creep strains, while silica fume was efficient in reducing shrinkage strains. Houge [22] found that the addition of 10% silica fume in concrete mixtures led to a substantial reduction in drying shrinkage. This is in good agreement with the results of the present study (Figure 3b). Carette and Malhotra [23], however, reported that concrete containing silica fume generally had drying shrinkage comparable to the control concrete, while Luther and Hansen [24] concluded that the drying shrinkage of high-strength silica fume concrete was either equal to or lower than that of concrete mixtures of equal strength without silica fume.

Trass concrete specimens (TL and TC) and plain concrete (PC1) exhibited higher shrinkage strains in comparison to other specimens. Several reports have indicated that the creep and shrinkage deformations of high-strength concrete are lower than those of normal-strength concrete. This is thought to be due to the dense matrix and low water-cementitious materials ratio [13]. It was observed that SFC1, which had the highest compressive strength, exhibited the lowest shrinkage strains, but the highest creep strains. Slag had only a minor effect on shrinkage and the difference in the results was within the intrinsic scatter of concrete shrinkage (10 to 15%). In contrast to slag, the addition of trass slightly increased the shrinkage of the concrete. This may be related to the ability of trass to influence the shrinkage mechanism, which could adversely affect the increase of shrinkage strains.

Laboratory conditions of temperature and relative humidity were monitored during creep and shrinkage measurements of PL, TL and SFL specimens after curing, as shown in Figures 5a and 5b, in order to assess their

effect on the creep and shrinkage of the specimens.

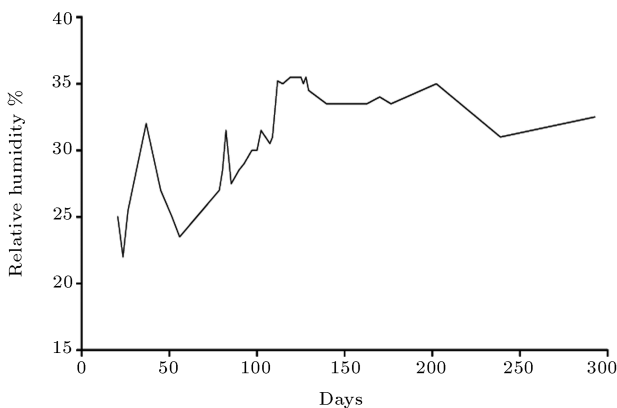


Figure 5a. Relative humidity changes of laboratory.

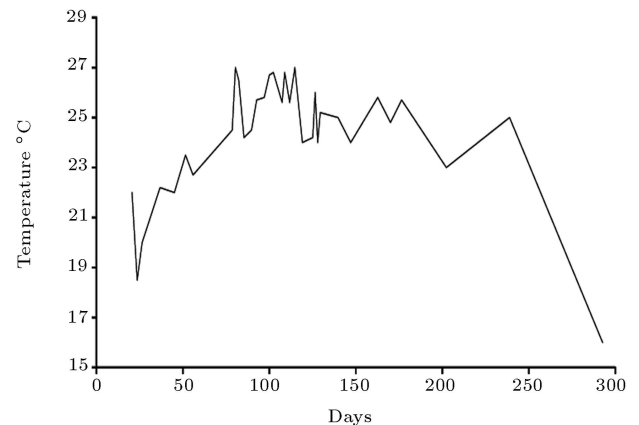


Figure 5b. Temperature changes of laboratory.

It was clearly observed that the creep and shrinkage of concrete specimens were sensitive to the temperature and relative humidity of the laboratory ambient condition. Fluctuations were indicated by the measured creep and shrinkage values. It was noted, however, that the creep and shrinkage of concrete specimens are higher for the higher temperature and lower relative humidity. The creep, at a temperature of 40°C , was higher than that at a temperature of 20°C . The creep was not highly sensitive to the relative humidity encountered in this study. The results indicated that a 20% difference in the relative humidity of two ambient conditions did not lead to a significant decrease in creep strains. Shrinkage values of concrete specimens under controlled conditions were lower than that of those under laboratory conditions. The decrease of shrinkage strains from 30 to 50%, due to a relative humidity increase of 20%, was more considerable than the increase of increasing shrinkage, due to a temperature increase of 20°C , from 20 to 40°C . It can thus be concluded that the shrinkage is more sensitive to relative humidity than temperature.

To verify the accuracy of the models, the predicted creep and shrinkage values (at 120 and 200 days after curing) were compared with the measured data. The predicted values of creep and shrinkage, using the ACI209-92, BS8110-1986, CEB1970 models and estimations based on 28-day results (short-term test method) are listed in Tables 8 to 12 and compared with the test results of specimens for mixtures. Most of the test results for creep and shrinkage strains are higher than the values predicted by these models. 28-day results (short-term test method) showed a relatively better prediction of creep and shrinkage strains. The accuracy of the prediction of creep can be considerably improved by undertaking short-term tests of 28-days duration and then extrapolating the results to obtain long-term values. The following equations relate the value of creep, c_t , at any time, t , after the start of loading to the value of creep after 28 days, c_{28} , under

Table 8. 120-day creep values based on tests and standards (microstrain).

Concrete Code	ACI	BS	CEB	Estimates Based on 28-Day Results	Lab. Results
PL	512	839	762	889	720
TL	767	1262	1148	711	856
SFL	499	822	747	1317	780
PC1	442	747	669	1625	1234
TC	648	1098	984	1471	1300
SFC1	444	78	670	1134	1380
SC1	696	1091	990	992	860
SC2	718	1221	1093	1479	1210
SFC2	447	750	983	1157	1330

Table 9. 200-day creep values based on tests and standards (microstrain).

Concrete Code	ACI	BS	CEB	Estimates Based on 28-Day Results	Lab. Results
PL	564	930	846	972	760
TL	850	1399	1273	778	900
SFL	553	912	829	1421	1160
PC1	489	829	743	1777	1425
SFC1	492	829	743	1276	1695
SC1	759	1197	1086	1085	1000

Table 10. 120-day shrinkage values based on tests and standards (microstrain).

Concrete Code	ACI	BS	CEB	Estimates Based on 28-Day Results	Lab. Results
PL	504	319	318	928	980
TL	504	319	318	1122	1310
SFL	504	319	318	978	720
PC1	413	298	281	1228	1000
TC	413	298	281	1088	1200
SFC1	413	298	281	775	892
SC1	413	298	281	1048	1020
SC2	413	298	281	1008	980
SFC2	413	323	642	928	1100

Table 11. 200-day shrinkage values based on tests and standards (microstrain).

Concrete Code	ACI	BS	CEB	Estimates Based on 28-Day Results	Lab. Results
PL	557	352	351	965	1100
TL	557	352	351	1159	1420
SFL	557	352	351	1015	1130
PC1	456	328	310	1265	1180
SFC1	456	328	310	815	919
SC1	456	328	310	1085	1150

Table 12. 120-day creep and shrinkage values based on tests and standards (microstrain).

Concrete Code	ACI	BS	CEB	Estimates Based on 28-Day Results	Lab. Results
PL	1016	1158	1080	1817	1700
TL	1271	1581	1466	1833	2166
SFL	1003	1141	1065	2295	1500
PC1	855	1045	950	2853	2234
TC	1061	1396	1265	2559	2500
SFC1	857	1046	951	1909	2272
SC1	1109	1389	1271	2040	1880
SC2	1131	1519	1374	2487	2190
SFC2	860	1073	1625	2085	2430

loading.

For sealed or saturated concrete:

$$c_t = c_{28} \times 0.5 t^{0.2}. \quad (1)$$

For drying concrete:

$$c_t = c_{28} \times [-6.19 + 2.15 \log_e t]^{\frac{1}{2.64}}, \quad (2)$$

where t is the time under load in days > 28 days.

Similar to creep, the shrinkage of both normal and light weight concretes stored in any drying environment at normal temperatures can be expressed as follows:

$$\varepsilon_{sh}(t, \tau_0) = \varepsilon_{sh28} + 100 \times [3.61 \times \log_e(t - \tau_0) - 12.05]^{\frac{1}{2}}, \quad (3)$$

where $\varepsilon_{sh}(t, \tau_0)$ is long-term shrinkage (10^{-6}) at age $t + \tau_0$ with τ_0 being the drying age; ε_{sh28} is shrinkage (10^{-6}) after 28 days; and $(t - \tau_0)$ is the time since the start of drying (> 28 days).

It was also observed from the test results of the mixtures that pozzolanic materials lead to an increase in the creep and shrinkage values of concrete. The type and content percentage of pozzolan had major effects on creep and shrinkage, especially for concrete mixtures that had a content of silica fume and trass.

The ranges of measured creep and shrinkage strains at 120 and 200 days were substantially more than those predicted by the ACI209-92, BS8110-1986 and CEB1970 prediction models. For SFC1, measured creep strain at the age of 200 days was 1695 microstrains versus 492, 829 and 743 microstrains predicted by the models, respectively. Measured shrinkage at the same age was 919 microstrains versus 456, 328 and 310 microstrains predicted by the ACI209-92, BS8110-1986 and CEB1970 models, respectively. Larger errors in predicting the creep and shrinkage of concrete

with pozzolanic material content indicate that a more sophisticated model of creep and shrinkage is required, taking into account the effect of pozzolanic material content on the time function. If accurate predictions of deformations are required, creep and shrinkage must be measured on the prototype concrete and extrapolated for the prediction of long-term behavior.

Relatively high initial rates of shrinkage and creep of high-performance concrete containing pozzolanic materials have also been reported. The ACI209-92, BS8110-1986 and CEB1970 models, based on the data from normal-concrete, have been used for the prediction of creep and shrinkage strains since the 1970s. Although these models include the effects of many significant factors, they have not taken into consideration the effect of pozzolanic materials in concrete. The use of these models, therefore, could lead to inaccurate prediction of the creep and shrinkage of high-performance concrete containing pozzolanic materials. It has been shown here that models (based on a concrete mixture) cannot accurately predict the creep and shrinkage for different concrete mixtures because of the variability of material properties, while predictions based on short-term tests using 28-day results lead to more reliable creep and shrinkage values at the desired times.

CONCLUSIONS

Based on the experimental and analytical results presented in this paper, the following conclusions and recommendations could be made.

The effect of additives, such as pozzolanic material, is not accounted for in creep and shrinkage time functions. To predict long-term creep and shrinkage strains from short-term results, the tests should be carried out on concrete without pozzolans. More accurate time functions should be developed to account

for the effect of pozzolanic material contents in the concrete mixtures.

The results of creep and shrinkage predictions in this study indicated that the ACI, BS and CEB models could not accurately predict the creep and shrinkage of pozzolanic concrete, because the creep and shrinkage of the concrete were affected by the type and content of pozzolanic materials in the mixture. The best way to determine the long-term creep and shrinkage of a specified mixture is to conduct short-term tests and use short-term test methods to predict these values.

The predicted creep and shrinkage strains using the 28-day results (short-term test method) are more accurate than predictions using any of the ACI209-92, BS8110-1986 and CEB1970 models.

The analysis and comparison of the test results of concrete with silica fume and plain concrete showed that the creep and shrinkage of silica fume concrete were higher than those of plain concrete under laboratory ambient conditions. It was also noticed that the creep and shrinkage strains of silica fume and trass concrete tended to develop rapidly at the early age of the concrete, compared to that of plain concrete under ambient conditions.

Under laboratory ambient conditions, concrete mixtures of trass content showed a higher creep for early ages up to approximately 40 days, after which the opposite was true, while the shrinkage strains of trass concrete were higher than plain concrete at all ages. Under controlled ambient conditions, ground-granulated blast-furnace slag concrete mixtures showed smaller creep in compression than other concretes. A 30% replacement level of slag caused a greater reduction in creep strains than that caused by a 15% slag replacement. The increase in the replacement level of slag, however, led to an increase in the shrinkage of concrete.

Experiments showed that higher temperature and lower relative humidity lead to the higher creep and shrinkage of concrete specimens. The creep was seen not to be highly sensitive to the relative humidity variation considered, while it was shown to be considerably sensitive to the temperature. The shrinkage values were lower under controlled ambient conditions than those under laboratory ambient conditions during the period of testing up to 200 days. It was also shown that the shrinkage was more sensitive to relative humidity than temperature.

ACKNOWLEDGMENTS

This project was supported by the Scientific Research Association of Iran at the Center (BHRC) under Grant No. 4790. The experimental tests were performed at the laboratories of the center. The contents of

this paper reflect the views of the authors and do not necessarily represent the views of BHRC.

REFERENCES

1. Goodspeed, C.H., Vanikar, S. and Cook, R.A. "High-performance concrete defined for highway structures", *Concrete International*, **18**(2), pp. 62-67 (February 1996).
2. Neville, A.M. and Brooks, J.J. "Concrete technology", *Longman Scientific & Technical* (1987).
3. Neville, A.M. "Properties of concrete", *Longman Scientific & Technical* (1995).
4. Wittmann, F.H. "Creep and shrinkage mechanisms", *Creep and Shrinkage in Concrete Structures*, Z.P. Bazant and F.H. Wittmann, Eds., John Wiley & Sons Ltd., Great Britain, pp. 129-161 (1982).
5. ACI Committee 209, *Prediction of Creep, Shrinkage, and Temperature Effects in Concrete Structures*, American Concrete Institute, Farmington Hills, Mich., p. 47 (1992).
6. British Standard, *Structural Use of Concrete*, BS8110 (1986).
7. Comite European du Beton (CEB), *Model Code for Concrete*, CEB (1970).
8. Lecture Notes of UNDP Experts, *Influence of Creep on Design, Performance and Safety of Concrete Dams*, A.A. Balkema and Rotterdam, India (1994).
9. Gardner, N.J. and Zhao, J.W. "Creep and shrinkage revisited", *ACI Materials Journal*, **90**(3), pp. 236-246 (May-June 1993).
10. Bazant, Z.P. and Baweja, S. "Creep and shrinkage prediction model for analysis and design of concrete structures- model B3", *Materials and Structures*, **28**(180), pp. 357-365, 415-430 and 488-495 (1995).
11. Bazant, Z.P. and Baweja, S. "Improved prediction model for time-dependant deformations of concrete", *Materials and Structures*, **24**, pp. 327-345 (1991).
12. Vandewalle, L. "Concrete creep and shrinkage at cyclic ambient conditions", *Cement and Concrete Composites*, **22**(3), pp. 201-208 (June 2000).
13. Sharon Hou, X., Al-Omaishi, N. and Tardos, M.K. "Creep, shrinkage and modulus of elasticity of high-performance concrete", *ACI Materials Journal*, **98**(6), pp. 440-449 (November-December 2001).
14. Neville, A.M., Dilger, W.H. and Brooks, J.J. "Creep of plain and structural concrete", *Construction Press* (1983).
15. Whiting, D.A., Detwiler, R.J. and Lagergren, E.S. "Cracking tendency and drying shrinkage of silica fume concrete for bridge deck applications", *ACI Materials Journal*, **97**(1), pp. 71-77 (January-February 2000).
16. Ojdrovic, R.P. and Zarghamee, M.S. "Concrete creep and shrinkage prediction from short-term tests", *ACI Materials Journal*, **93**(2), pp. 169-177 (March-April 1996).

17. Li, H., Wee, T.H. and Wong, S.F. "Early-age creep and shrinkage of blended Cement concrete", *ACI Materials Journal*, **99**(1), pp. 3-10 (January-February 2002).
18. Fulton, F.S. , *The Properties of Cement Portland Containing Milled Granulated Blast-Furnace Slag*, Portland Cement Institute, Johannesburg, pp. 4-46 (1974).
19. Hogan, F.J. and Meusel, J.W. "Evaluation for durability and strength development of a ground-granulated blast-furnace slag", *Cement, Concrete and Aggregates*, **3**(1), pp. 40-52 (1981).
20. Klieger, P. and Isberner, A.W. "Laboratory studies of blended cement-portland blast-furnace slag cements", *Journal of PCA Research and Development Laboratories*, **9**(3), pp. 2-22 (September 1967).
21. Altoubat, S.A. and Lange, D.A. "Tensile basic creep: Measurement and behavior at early age", *ACI Materials Journal*, **98**(5), pp. 386-393 (Sept.-Oct. 2001).
22. Haque, M.N. "Strength development and drying shrinkage of high-strength concrete", *Cement and Concrete Composites*, **18**(5), pp. 333-342 (October 1996).
23. Carette, G.G. and Malhorta, V.M. "Mechanical properties, durability and drying shrinkage of Portland cement concrete incorporating silica fume", *Cement, Concrete and Aggregates*, **5**(1), pp. 3-13 (1983).
24. Luther, M. and Hansen, W. "Comparison of creep and shrinkage of high-strength silica fume concretes with fly ash concretes of similar strengths", *Proceeding of the CANMET/ACI 3rd International Conference on the Use of Fly Ash, Silica Fume, Slag and Natural Pozzolans in Concrete*, SP-114, **1**, M. Malhorta, Ed., American Concrete Institute, Farmington Hills, Mich., p. 18 (1995).